The Origin of Shear Turbulence

Horia DUMITRESCU[1], Vladimir CARDOS*,[1]

*Corresponding author
[1]"Gheorghe Mihoc – Caius Iacob" Institute of Mathematical Statistics and Applied Mathematics of the Romanian Academy,
Calea 13 Septembrie no. 13, 050711 Bucharest, Romania,
dumitrescu.horia@yahoo.com, v_cardos@yahoo.ca*

DOI: 10.13111/2066-8201.2017.9.4.7

Received: 02 October 2017/ Accepted: 23 October 2017/ Published: December 2017

Abstract: *Previously, the turbulent flows were studied as they have been disregarding their origin, and without looking into some of the details of the mechanism of turbulence production and sustainment. This approach focusing its attention particularly on the details of the fluctuating motion superimposed on the main motion led to most of controversial and misunderstood results from which the law of equal action and reaction, and the circulation-conserving were excluded. The paper is aiming at removing these drawbacks and presenting the turbulence phenomenon as a mechanical process triggered off at the beginning of motion. The fluid as deformable continuum without a definite shape must be guided by some physical surfaces, where the rotor-translational motion approximation is more suited than the no-acceleration parallel flow approximation. The main features of shear turbulence are described by means of the mechanical prototype of a perturbed rotor-translational motion continuously self-accelerating at wall and conserving the mass and angular momentum.*

Key Words: *Laminar-turbulent transition, Shear turbulence, Rotor-translational flow model.*

1. INTRODUCTION

Any motion, both of solids and fluids that starts from rest is the result of an impact process occurring during the momentum exchange between two colliding bodies within a short time of contact. This kind of collision will be called starting impact in the sequel. With respect to a single impacted body or structure, the loading in such a process acts with high intensity during this short period of time. As a result, the initial velocity distribution is rapidly changed inducing locally pressure wave loadings. Such rapid loading in the contacting area is a source where waves are emitted and that propagate with finite speeds through the body. In the case of sufficiently small amplitudes (in the far field), linear elastic body waves propagate with the speed of sound waves. In the near field, if the body force is absent/ unimportant or has the analogous representation by means of the Helmholtz force potentials $\mathbf{k} = \operatorname{grad} b + \operatorname{curl} \mathbf{B}$, the local perturbation propagates as a wave packet/group at the interface of bodies containing the fast longitudinal L-waves and the slower transverse T-waves [1]. However, a further complication arises when the impact is a ballistic type one that acts on the micro structural change with non-Gaussian behavior of the molecular thermal agitation/energy [2]. In the near field large deformations with non-linear material behavior occurred that may even render fracturing of solid material and turbulence of fluids. The

impact problems are similar for both solids and fluids with the difference that the dispersion/inertia waves encountered in the wall-bounded turbulent flows complicate the pattern [3].

Within an idealized theory of the impact process, the rate form of the conservation laws by time integration and through the limit of vanishing duration of the loading is transformed to a set of finite difference relations. Their application is illustrated by the wave packets in an elastic rolling wheel and a boundary layer on a flat plate. Considerations of these typical examples give some insight into actual problems and, in an informal manner, yield some justification/interpretation of confused hairpin vortex structures in wall turbulent flows [4].

2. THE KINEMATICS AND KINETICS OF BODIES WITH ROTOR-TRANSLATIONAL MOTION

The gross properties of solids, liquids and gases are directly related to their molecular structure and to the nature of the force between the molecules. It is possible to distinguish two kinds of force which act on matter in bulk. In the first group are long-range force like gravity which decreases slowly with increase of distance between interacting elements/ molecules and which are still appreciable for distances characteristic of natural fluid flows. Long-range forces are also called volume or body forces.

In the second group there are short-range forces, which have a direct molecular origin, decrease extremely rapidly with increase of distance between interacting elements, and are appreciable only when that distance is the order of the separation of molecules of the solid/fluid. They are called surface/shear forces and are negligible unless there is direct mechanical contact between the interacting elements, as in the case of reaction/collision between two rigid bodies. But, in the case of starting impact/collision the short-range forces exerted between two deforming bodies, in contact at their common boundary, are due predominantly to transport of momentum across boundary by migrating molecules: from warmer body to colder body. The intrinsic/molecular-thermal energy involved in this molecular process may thus also be called "latent heat" of compressing. In the case of sharp loading, the energy dissipated cyclically through internal/molecular friction increases the amplitude of nonlinear instabilities (turbulence of flowing fluids). The self-vibrating mechanical systems with nonlinear restoring forces and nonlinear/hysteretic damping have originated from micro-structural changes of materials, during the starting impact where the structural damping is characteristic of all systems with hysteretic cycle (particularly turbulence of flowing fluids). The shear forces activated by the starting impact act on matter in bulk at the onset of a motion, occurring dissipative molecular-thermal effects, less or more pronounced, from simple dry friction forces (frictional shearing stress) up to nonlinear restoring forces with hysteretic damping (turbulence), depending on the intensity of starting impact, Fig. 1.

The first cornerstone of the rotor-translational motion is the starting impact triggering off a motion, that is idealized by a sudden jump of kinetic energy, $E_0 = 1/2mV_0^2 = 1/2I_{IRC}\omega^2$, equal-partitioned into translational motion and rotational motion and described by a Dirac function $E(t) = E_0\delta(t-a), t \geq a$. During this starting short period of time a potential energy E_0 is stored as the internal molecular-thermal energy of micro-structure of moving solid/fluid like a "latent heat" of compressing (the work of the internal shear forces in the time interval elapsed). After impact, the development of motion depends on the intensity of the starting impact: for an inelastic impact the colliding bodies

separate immediately and the "latent heat" of compressing, E_p, is dissipated as drag friction, Fig. 1a, for an elastic/linear impact, there is only neglected rolling friction, the contact point describes a cycloidal trajectory and the molecular thermal energy sustains instabilities/vibrations of the moving body, firstly linear torsional vibrations, Fig. 1b, followed for higher intensity by nonlinear coupled vibrations with structural damping and microstructure changes of materials, Fig. 1c.

a)

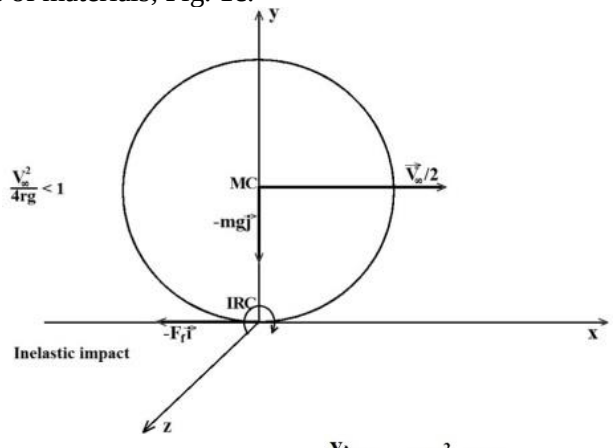

b)

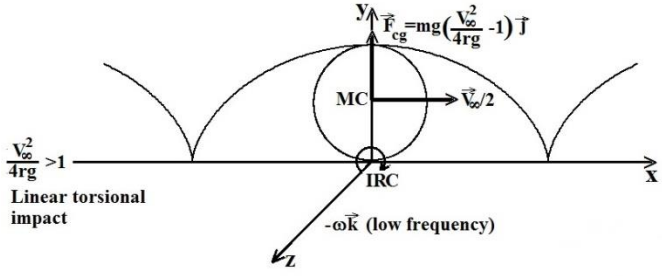

c)

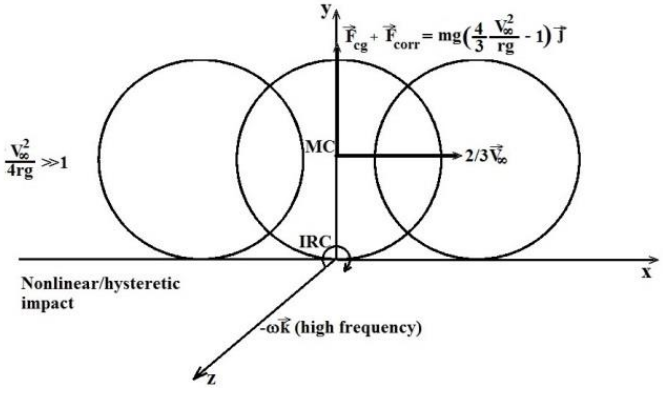

Figure 1 – Starting impact types

The second crucial feature of starting impact is that the strong contraction of motion, $\delta(t-a)=1$ at $t = a$, can be interpreted by means of the elementary affine transformations of Cantor's set: a first time contraction in a proportion of 1/3 (equal to Fourier coefficient $B(\omega)$) and a second contraction in the same proportion of 1/3 (a rotation) followed by a translation of 2/3, showing the rest-motion passing way by accelerating rotor-translational movements. The passing from the boundary rotation motion with constant angular momentum (rotational invariance) to a free translational motion with constant momentum (translational invariance)

involves always a buffer zone/boundary layer for the damping of strong boundary accelerations induced by the starting process. If the body forces are absent/unimportant or have a Helmholtz-like representation $\mathbf{k} = \text{grad}\, b + \text{curl}\, \mathbf{B}$, the bodies, solids and/or fluids, can perform continuously accelerating rotor-translational motions with light damping after impact. When the starting conditions are sufficiently severe some instability state sets in, which is followed by further (secondary, tertiary, …) instabilities (bifurcations); in the case of fluids the transition and a fully developed turbulent state are set in. Such sequences of events depending on the starting conditions originate locally in the contact/impact point and then are spatially developing throughout the whole motion field. It is important to stress that the transition from origin point to a vibration/turbulent regime may be quite sudden, however, the boundary rotor-translation turbulent motion induces an rotation inertial delay (unimportant for solids but vital for turbulence). Thus, the mechanical prototype of the rotor-translational like movements illustrated by the wheel/disk in a straight rolling motion shows unexpected many similarities with the streaklines in a boundary-layer flow with travelling instability waves [5].

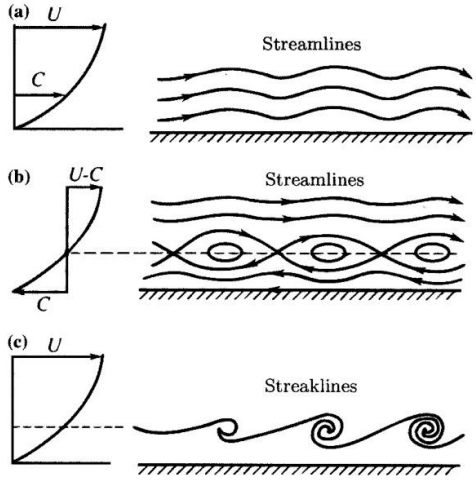

Figure 2 – Streamlines and streaklines in a boundary layer with travelling instability waves [5]

Figure 2 sketches the unsteady streamlines and streaklines containing various instabilities depending on the degree of concentration of the boundary vorticity [6], [7] Fig. 3.

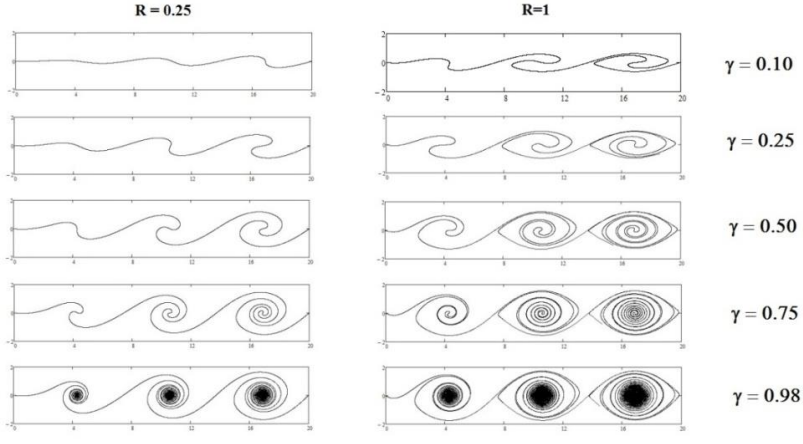

Figure 3 – Effect of concentrated boundary vorticity on streakline patterns [6]

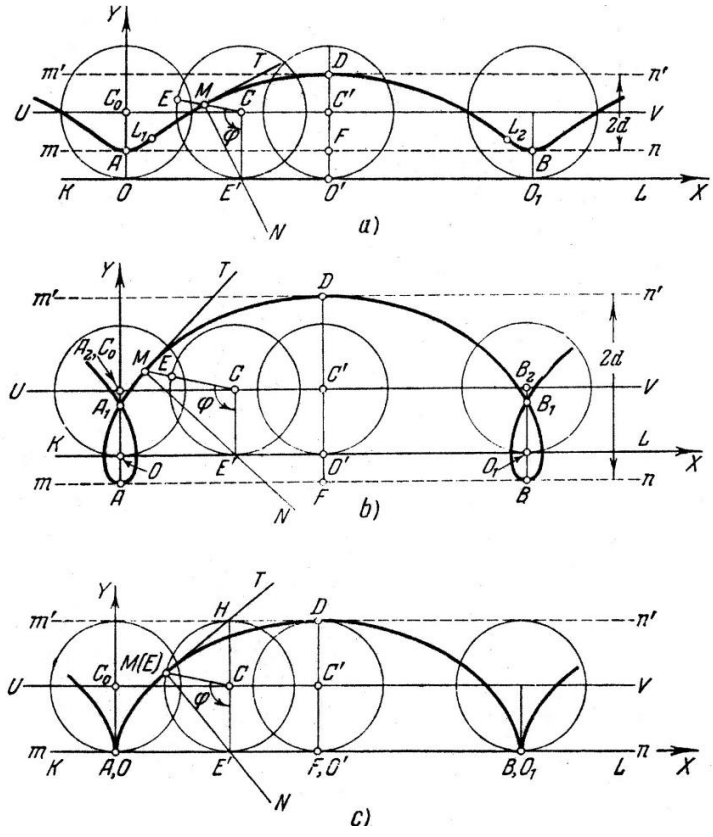

Figure 4 – Typical cycloidal trajectories: a) short cycloid, b) long cycloid, c) ordinary cycloid

Such as cat-eyes like structures and streaklines can be easily obtained through the deformation of the cycloidal trajectory/path described by a no slip rolling disk. When the impact point M is not on the girth of the disk, this point describes a deformed cycloid: if M is inside $CM = d < r$ (r-radius of disk) the cycloid is a short one (Fig. 4a), and if M is outside $d > r$ the cycloid is long one (Fig. 4b). For $d = r$, the point M describes an ordinary cycloid (Fig. 4c), which can deviate less or more from the typical form depending on the intensity of collision/impact, Fig. 1.

From the parametric equations of the cycloid

$$x = r\varphi - d\sin\varphi,\ y = r - d\cos\varphi, \tag{1}$$

the peripherical velocity and centripetal acceleration are directly found as

$$\frac{V^2(\varphi)}{r^2\omega^2} = \left(1+\lambda^2\right)\left(1-\frac{2\lambda\cos\varphi}{1+\lambda^2}\right),\ \lambda = \frac{d}{r}, \tag{2}$$

$$\frac{a_n}{r\omega^2} = \lambda, \tag{3}$$

where the angular velocity has a constant line of action, i.e. $\boldsymbol{\omega} = \omega(t)\mathbf{i}_z$.

For the initial conditions $\varphi = \pi$ and $r\omega = V_\infty/2$ from Eqs 2, 3 it can define an impact coefficient as

$$C_I \equiv \frac{V_{\max}^2}{ra_n} = \frac{V_\infty^2}{4gr} = \frac{(1+\lambda)^2}{\lambda}, \tag{4}$$

where g is the acceleration of gravity and the critical value $\lambda_0 = 1$ corresponding to $C_I = 4$ or $V_\infty = 4\sqrt{g} = 12.528$ m/s with reference radius r = 1 m, is the starting minimum condition for the rotor-translational motion with ordinary cycloidal trajectory.

For $\lambda \le \lambda_1$, the long/deformed cycloid contains knots (intersection points with the straight lines $x = 2k\pi r$, k is whole number) obtained from the equation

$$\varphi - \lambda \sin\varphi = 0, \tag{5}$$

where λ_1 = 4.60333 is the value corresponding to the smallest positive root of Eq. (5) and $C_I = 6.8174$ or $V_\infty = 16.356$ m/s.

The impact in the range $\lambda_0 \le \lambda \le \lambda_1$, is an inelastic one without microstructural change where the molecular thermal agitation/energy is not affected by the rolling friction, and at the macroscale the motion obeys the Konig's paradigm: the kinetic energy is the sum of the translational kinetic energy and of the rotary energy mass being concentrated in the mass center.

The value λ_1 is equal with the Feigenbaum's criterion (4.669…) [8] indicating the onset of an instability state at the molecular scale. From the equation

$$\varphi - \lambda \sin\varphi = \pi, \tag{6}$$

new knots are found on the straight lines $x = (2k+1)\pi r$ as a point-couple for each line $(P_1, P_2), (Q_1, Q_2), (R_1, R_2)$, Fig. 5, where $\lambda_2 = 7.78968$ is the value corresponding to the smallest positive root of Eq. (6), and $C_I = 9.9184$ or $V_\infty \cong 20$ m/s.

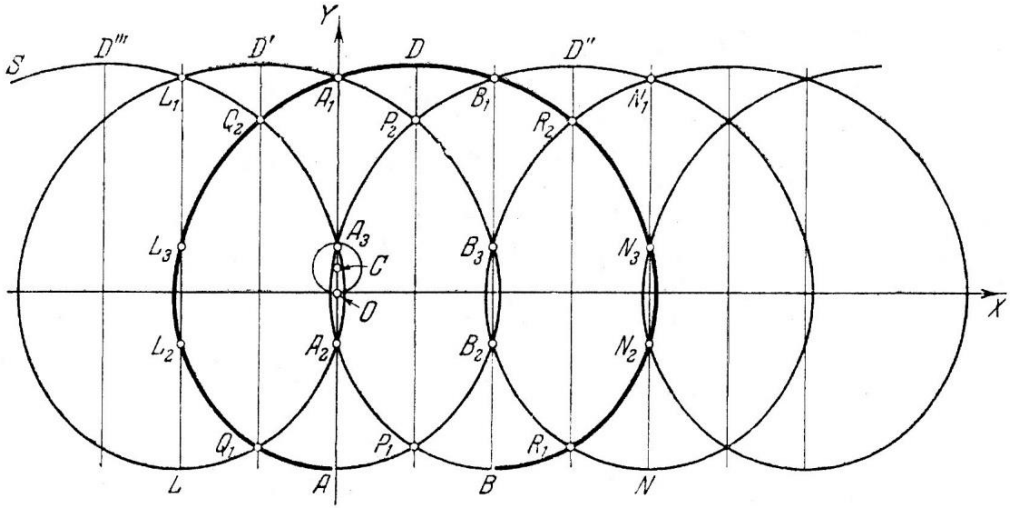

Figure 5 – Cycloidal trajectories in critical regimes

The impact in the range $\lambda_1 < \lambda \le \lambda_2$ is a linear elastic/random impact preserving the Gaussian behavior of the molecular macrostructure without inertia changes/deformations at

the macroscale. After impact, the motion of the elastic disk is given by a Konig-like paradigm as

$$E_k = \frac{m}{2}\bar{V}_M^2 + \frac{1}{2}I_M\omega^2, \tag{7}$$

using the average velocity per one rotation, $\bar{V}_M = 2/3V_\infty$ and $\omega r = \sqrt{2/3}V_\infty$.

Its vibration state depending only on the impact energy E_0 is described by a linear slightly damped torsional oscillator of mass *m* and stiffness of the restoring torsional spring *c* with the initial velocity $V_\infty, E_0 = \frac{1}{2}mV_\infty^2 = I_{IRC}\omega_0^2$. The un-damped free vibration motion of the disk is the solution of equation, Fig. 6.

$$\ddot{\alpha} + \omega_0^2\alpha = 0, \quad \omega_0 = \sqrt{\frac{e}{m}i_s^2}, \quad i_s = \sqrt{\frac{I_{IRC}}{m}},$$

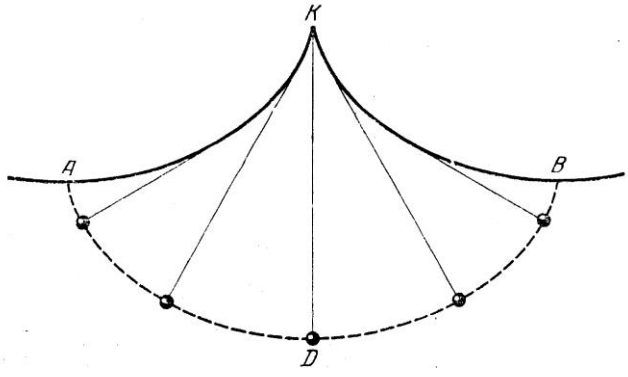

Figure 6 – Linear-torsion oscillator regime after a random impact ($\lambda_1 \le \lambda < \lambda_2$).

Conservation of energy applies at any instant of time and gravity has no influence on the natural vibration

$$E_k + E_p = E_0 = \frac{1}{2}mV_\infty^2, \tag{8}$$

where the translational kinetic energy E_k vanishes (E_k =0) and the rotation inertial potential is maximum ($E_p = E_{p\max} = 1/2I_{IRC}\omega_0^2 = E_0$) for $t = 0, \pi/\omega_0, 2\pi/\omega_0$ and contrary $E_k = E_{k\max} = \frac{m}{2}V_\infty^2 = E_0$ and $E_p = 0$ for $t = \frac{\pi}{2}\omega_0, \frac{3\pi}{2}\omega_0, \ldots$ (Rayleigh's quotient [1]).

If the rotation frequency ω_0 approaches the critical frequency ω_c, the material damping cannot be neglected and the dispersion waves by the lateral inertia must be considered.

In the interval $\varphi \in [2\pi, 3\pi]$ for $\lambda_2 < \lambda \le \lambda_3$, through Eq. 5, the cycloid acquires new double knots on the straight lines $x = 2k\pi r : (A_2, A_3)$, on $x = 0$, (B_2, B_3), on $x = 2\pi r$, (L_2, L_3), on $x = -2\pi r$, etc., Fig. 5, where $\lambda_3 = 14.102$ $(C_I = 16.171$ and $V_\infty = 25.433)$.

For $\lambda > \lambda_2$, the impact is a nonlinear/ballistic impact involving irreversible/hysteretic microstructure changes with nonlinear material behavior (or non Gaussian behavior of the

molecular thermal energy), that lead to the changes at the macro-scale, with structural hysteretic/damping and inertial dispersion wave (Fig. 7).

The kinetic energy of a deformed body is given by

$$E_k(t) = \frac{m}{2}\bar{V}_M^2 + \frac{1}{2}\boldsymbol{\omega}^T \boldsymbol{I}\boldsymbol{\omega}\,, \tag{9}$$

where the kinetic energy becomes the sum of the translational kinetic energy (mass is considered to be concentrated in the mass center) and of the rotary energy.

With respect to principal axes, the later is given by (the inertia tensor is diagonal)

$$\frac{1}{2}\boldsymbol{\omega}^T \boldsymbol{I}\boldsymbol{\omega} = \frac{1}{2}\left(I_z\omega_z^2 + I_x\omega_x^2 + I_y\omega_y^2\right)$$

Using the Lorenz curve [8], [9], [10] for the distribution of rotary energy, Eq. (9) becomes

$$E_k = \frac{m}{2}\bar{V}_M^2 + \frac{1}{2}I_M\omega^2\left(1+G\right), \tag{10}$$

where $G = \dfrac{I_x\omega_x^2 + I_y\omega_y^2}{I_z\omega_z^2} = \dfrac{1}{3}$ is the Gini coefficient [11], $\bar{V}_M = 2/3V_\infty$ and $\omega r/V_\infty = \sqrt{2/3}$.

In the case of sharp loading of a disk of a material sensitive to tension, tensile fracture may occur despite original loading in compression, due to the sign change during reflection of the dispersion wave ("spalling effect").

The cycloid curve has some interesting geometrical properties related with above instabilities induced by motion of bodies describing such trajectories.

Thus, the ratio of arc of ordinary cycloid to circular arc, $4/\pi$, and the area swept by cycloid to circular area, 3, show that the accelerating cycloidal motion can smooth out the translation-rotation phase difference, induced during the starting impact, by the increase of frequency and/or the rotational inertia decreasing.

Also, the area generated by the rotation of a cycloid around its height (DF) can illustrate the vibration zone (see shaded area in Fig. 7c).

The instantaneous velocity and inertia distributions (Fig. 7a) across the traveling direction of the rolling wheel, can be approximated as $\dfrac{V(y)}{V_\infty} = \sin\dfrac{\theta}{2}$ and $\dfrac{I(y)}{I_{IRC}} = \cos^2\dfrac{\theta}{2}$ with $\theta = \omega t$ and

$$\underbrace{\left(\frac{V(y)}{V_\infty}\right)^2}_{E_k} + \underbrace{\frac{\omega^2 I(y)}{\omega^2 I_{IRC}}}_{E_p} = 2 + \frac{1}{4}\,, \tag{11}$$

where E_k is translational kinetic energy and E_p is rotary inertial energy.

The equation show the intrinsic flywheel mechanism of kinetic energy preserving in a slightly damped rotor-translational motion.

This motion induces an inertial potential around of the instantaneous rotation center, Fig. 7a, b where the oscillating inertia center is below the mass center and the value ¼ is the energy fraction dissipated per cycle by the structural damping. Equation (11) is a kind of Rayleigh's quotient [1] based Lorentz's distribution.

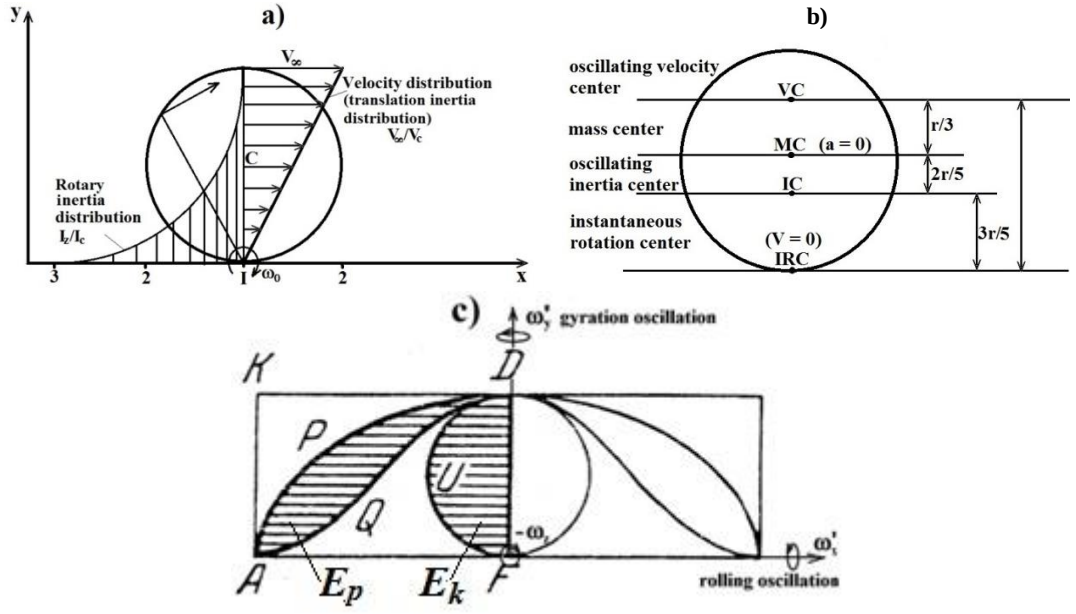

Figure 7 – Hysteretic behavior after a ballistic impact ($\lambda \geq \lambda_2 = 7.789$)

The equality of shaded areas from Fig. 6c, the petal AQDP and the half of generator disk, can be interpreted as the dynamic balance between E_p and E_k, that is assumed to be affine to their inertia, Fig. 7a.

3. SHEAR WAVES IN WALL-BOUNDED FLOWS

The considerations and interpretations herein concerning the shear waves previously found in boundary layer [3], [7], [12], [13], [14], are based on the references to the body waves (section 2). Among various shear layers, the thin boundary layers are final gross structures generated by and adjacent to solid surfaces during the onset of motion. The concentrated boundary vorticity (CRV) generated by the starting impact is a primary local structure [7] inducing travelling instability waves across the whole boundary layer non excluding three dimensional effects. The future evolution of CVB only depending on the present state (and not on this history), is described by a longitudinal compressing/expanding wave with a displacement in the direction of the main motion.

The CBV plays the role of the generator disk from the above cycloidal motion inducing instabilities. The local instabilities generated by CBV propagate across the whole boundary layer in the form of transverse shear wave packets containing an incident frictional shear wave and two reflected waves: elastic shear wave and dispersion shear wave, in opposite phase with the incident wave [14].

The importance of boundary layers consist in their rotation inertial potential that balances the transitional kinetic energy of main motion. For large Reynolds number exceeding the critical boundary value $R_{bcr} = l^2 e^2 \nu_0^{-1}$ [7] the starting impact is a ballistic-like impact that induces irreversible/hysteretic fluid micro-structure changes accompanied by an augmented molecular thermal energy feeding the shear wave system. The dynamic balance between the translational kinetic energy of main motion and the rotary inertial potential of the whole boundary layer is achieved by means of a self-sustaining shear wave system with

lower frequencies ($\mathrm{Re}_l^{1/2}$) called the self-sustaining mechanism of turbulence. In addition to this slow gross hysteretic cycle with the frequency about $\mathrm{Re}_l^{1/2}$ at the boundary layer scale (δ), there is a local faster molecular thermal process at the fluid-solid interface with the natural frequency of fluid, $\mathrm{Re}_{cr} \approx \nu_0^{-1}$.

Its augmented intrinsic/ molecular thermal energy supplies the energy at wall for the rotation inertial potential, that is a little out of sync with the less inertia translational kinetic potential. In contrast to the impulsive starting, the stress relaxation/damping after impact is achieved differently depending on three frequency levels: 1) high frequency ($\mathrm{Re}_{cr} \approx \nu_0^{-1}$) at fluid-solid boundary by means of the longitudinal wave and structural damping, i.e. internal/molecular friction involving micro-structure changes; 2) frequencies depending on Reynolds number ($\mathrm{Re}_l^{1/2}$) and distinct modes with small wave numbers ($k\delta = \pi/4, \pi/2, 2\pi/3$) by means of the nonlinear shear wave packets and nonlinear/hysteretic damping across the boundary layer; 3) frequencies depending on Reynolds number ($\mathrm{Re}_l^{1/2}$) and random modes with large wave numbers ($k\delta \approx 2\pi$) that transport Helmholtz like weak vorticity by viscous diffusion across the whole boundary layer.

The velocity field of both laminar and turbulent boundary layers are dominated by the bound conditions so that the details of the nonlinear fluctuating motion at large wave number and high frequency superimposed on the average motion is not contradictory to the translational invariance (momentum-preserving) and the latter can be decoupled by the rotational field of waves with small wave numbers and high frequency obeying the angular momentum-preserving, i.e. the rotational invariance.

Based on this wave number decomposition, the present approach of wall-bounded flows uses the similar solutions of the Navier-Stokes equations in the boundary-layer approximation associated with a mutual induction function, CBV-viscosity $\nu(\mathrm{Re}_l)$. Thus, the boundary layer playing the role of the rotation inertia must be associated with a relaxation/accommodation relation between the CBV and variable viscosity, self- adjusting with the flow state (thixotropic fluid hypothesis [7]) that determines the proper frequencies of wave system. For Prandtl boundary-layer flow, Blasius equation corrected with acceleration effect (α_4) given by the mutual induction factor (Fig. 8) becomes a soliton, which retain identity upon the flow-solid collision:

Corrected Blasius equation

$$\alpha_4 f''' + f f'' = 0, \tag{12}$$

Boundary conditions

$$\begin{aligned} &\eta = 0: \quad f = 0,\ f' = 1 \\ &\eta \to \infty: f' = 1 \end{aligned}, \tag{13}$$

Mutual induction factor

$$\begin{aligned} &\alpha_4 = e^{\tau},\ \tau \in \{2,1,0\} \ \text{ for } \mathrm{Re}_l < \mathrm{R}_{bcr} \ \text{ (weak coupling)} \\ &\alpha_4 = e^{-\tau},\ \tau \in \{2,1,1/2,1/4\} \ \text{ for } \mathrm{Re}_l \geq \mathrm{R}_{bcr} \ \text{ (strong coupling)} \end{aligned}, \tag{14}$$

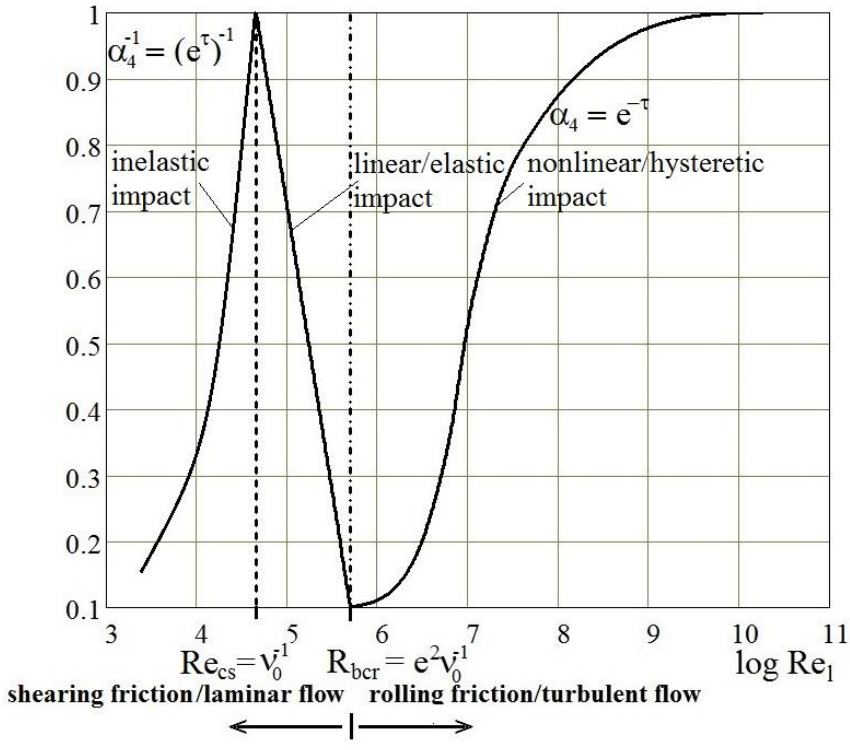

Figure 8 – The mutual induction factor $\alpha_4(\mathrm{Re}_l)$

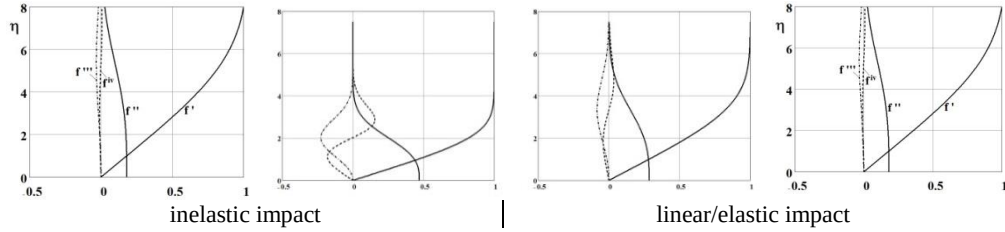

Laminar flows $(l = 1m)$; $R_b / l^2 =$

$e^2\nu_0^{-1/2} \approx 2\cdot 10^3$	$e^0\nu_0^{-1} \approx 10^5$	$e\nu_0^{-1} \approx 2\cdot 10^5$	$e^2\nu_0^{-1} \approx 5\cdot 10^5$

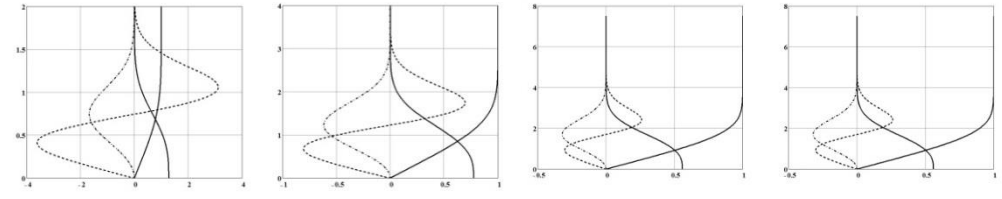

nonlinear/hysteretic impact

Transitional – turbulent flows $(U_b = 1m/s)$; $R_b / U_b^2 =$

$e^{-2}\nu^{-\left(1+\frac{1}{2}\right)} \approx 2\cdot 10^6$	$e^{-1}\nu_0^{-\left(1+\frac{1}{2}\right)} \approx 6\cdot 10^6$	$e^{-1/2}\nu_0^{-\left(1+\frac{1}{2}\right)} \approx 10^7$	$e^{-1/4}\nu_0^{-2} \approx 5\cdot 10^9$

Figure 9 – Similar soliton solutions of mean velocity and shear wave fields for the Prandtl boundary-layer flow

Figure 9 illustrates the superposition of velocity field with large wave number $(2\pi n, n \to \infty)$ on the shear wave field with small wave number $(\leq 2\pi)$ for different Reynolds numbers. The velocity field and wave field are consistent with translational invariance and rotational invariance, respectively. The longitudinal slight dispersion/damping of the CBV is of molecular nature and can be modelled by a near harmonic motion described by

$$g''(\xi) + \omega_0^2 \left[g(\xi) + s\,\mathrm{sgn}\, g'(\xi) \right] = 0, \tag{15}$$

where $g = e^{\tau}/e^2$ and *s* characterizes the frictional force by the limit of the spring force for the thixotropic like behaviour of fluid $\left(s = e^{-2}\right)$. The mutual induction between the CBV and the viscoelastic fluid produces a fast longitudinal compressing/expanding wave that propagates along the solid wall with high frequency near the natural frequency $\omega_c = U_b^2 \nu_0^{-1}$ $(\text{for } U_b = 1m/s)$ and has a lightly damped oscillating decay, Fig. 10.

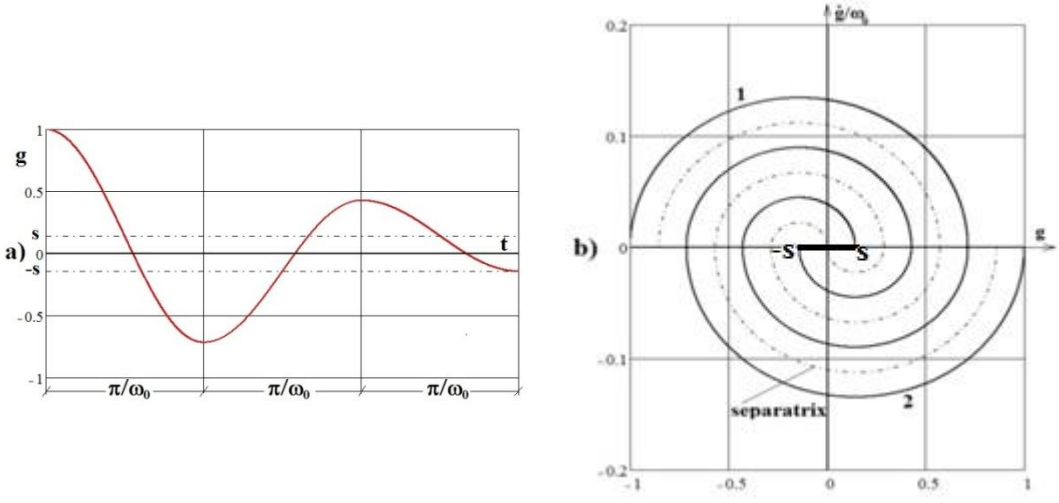

Figure 10 – The oscillating motion of CBV: a) longitudinal lightly damped wave in thixotropic fluid; b) phase curves and separatrix of frictional vibrations

The key mechanism of transverse dispersion/damping of the CBV is the boundary rotor-translational motion generating shear waves on independent modes with small wave number that penetrate the velocity field averaged on random large wave number-modes and by their coupling the boundary non-linearity/accelerations effect is offset. The penetrating process of vorticity waves from a fluid-solid boundary into the boundary-layer flow can be illustrated by a simple harmonic surface wave exponentially decaying with the distance y from the wall [14],

$$U(y,t) = U_e/\pi e^{-k_t y}\cos(nt - k_t y), n = \log \mathrm{Re}_l, k_t = \sqrt{\frac{n}{2\log \nu_0^{-1}}}, \tag{16}$$

where $U_e/\pi e^{-k_t y}$ is the amplitude decreasing outwards, $k_t y$ is a phase lag of wall-bounded flow compared to the fast surface motion of CBV, and *nt* is a kind of wave number, $nt \leq 2\pi$.

The velocity distribution for distinct wave numbers is shown in Fig. 11, indicating the presence of three shear wave packet for small wave numbers, where the frictional shear wave $(\pi/4rad)$ is in opposite phase with the elastic wave $(\pi/2\,rad)$ and the inertial dispersion wave $(2\pi/3\,rad)$. The penetration depth or attenuation length is equal to 2/3 δ (δ – boundary layer thickness) that is just the wave length of oscillation. The three wave structure is consistent with the soliton solutions from Fig. 9.

4. CONCLUSIONS

The particular examples considered herein have shown that the starting conditions play an important role in the development of the motion of both solids and fluids including turbulent flows. Any motion of both solids and fluids that starts from rest is the result of an impact process occurring during the momentum exchange between two colliding bodies within a short time of contact. With respect to single impacted body or structure, the loading in such a process acts with high intensity during this short period of time. The starting impact induces a rotational relativity towards the incoming/incident translational motion involving important consequences on the evolution of motion after impact. The key assumption of this analysis is the self accelerating rotor-translation motion of the impact point describing a cycloidal trajectory. The cycloid curve has some interesting geometrical properties related with the instabilities induced by the motion of bodies describing such trajectories. Thus, the ratio of arc of ordinary cycloid to circular arc, 4/π, and the area swept by cycloidal to circular area, 3, show that the accelerating cycloidal motion can smooth out the translation-rotation phase difference, induced during the starting impact, by the increase of frequency and/or the decreasing of rotational inertia. Also, the area generated by the rotation of a cycloid around its height (DF) can illustrate the vibration zone (see shaded area in Fig. 7c). The motion along a cycloid self-generates various instabilities depending on the intensity of starting impact. An impact coefficient/criterion has been devised and a classification of impact types has been done by means of this criterion. The field of a solid and fluid motion has been described at both macro and micro-scale showing the wave system accompanying motion.

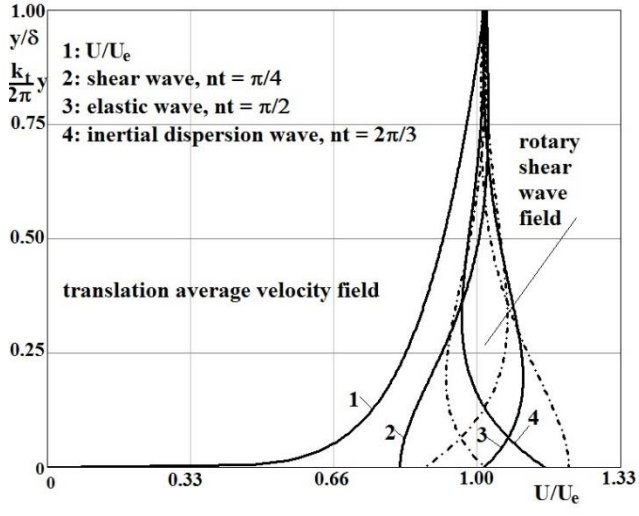

Figure 11 – The average velocity field (averaging on random modes with large wave numbers) and shear wave field (a superposition of three independent modes with small wave numbers

The two parallel examples of motions close to a solid surface have universal importance, so that, up to some yet be specified conditions, the results can be carried over the regions close to the wall of general turbulent flows. The main results of this study can be summarized as follows.

1. The onset of any flow generates three shear wave packets at the fluid-solid boundary moving with 2/3 of free velocity V_∞ called group/convection velocity; the result is known as the Taylor's frozen-field hypothesis; the transverse shear waves are governed by a modified Blasius equation/soliton, analogous to the KdV equation for solitary waves in shallow water, where the effects of boundary non-linearity will be offset only by the dispersion of CBV, without near-wall viscous dissipation.
2. The small wave number-Re_l depending on the frequency wall shear waves are mostly dispersing/damping across a thin boundary layer with non important viscous/dissipative effect on the velocity field averaged on large wave numbers; colloquially, the boundary vorticity dispersing flow is known as turbulent wake.
3. The turbulence mechanism without kinetic energy loss is a self-sustaining process supported by the molecular thermal energy released from fluid micro-structure changes during the starting impact ("latent heat" of compressing); it is a mechanical system with nonlinear restoring stresses and nonlinear/hysteretic light damping caused at a fluid-solid boundary by the starting impact.
4. The turbulence phenomenon has its origins at fluid-solid boundaries where localized singularities arise during the onset of motion and their effect propagates across the whole boundary layer (a dilemma of mathematicians: local versus integral [15]); the turbulence is characteristic to incompressible flows up to $M_\infty = 2/3$ (about half of the latent heat of compressing) and represents early compressibility effect: a stronger initial collision resulting in weakly attached microstructure elements is described by a new fluid state equation, $\frac{p}{\rho^\gamma} = const.$ with $\gamma = \frac{e}{2}$ as a remanent vorticity, i.e. early compressibility effects.

ACKNOWLEDGEMENT

This work was realized through the Partnership programme in priority domains – PN II, developed from ANCS CNDI – UEFISCDI, project no. PN-II-PT-PCCA-2011-32-1670.
This article is an improved version of the science communication with the same title, presented in *The 37th edition of the Conference "Caius Iacob" on Fluid Mechanics and its Technical Applications*, 16-17 November 2017, Bucharest, Romania, (held at INCAS, B-dul Iuliu Maniu 220, sector 6), *Section Plenary Lectures*.

REFERENCES

[1] F. Ziegler, *Mechanics of solids and fluids*, Springer-Verlag, New York, 1998.
[2] I. Corwin, Kardar-Paisi-Zhang (KPZ) universality, *EMS Newsletter*, No. 101, September, pp.19-27, 2016.
[3] J. Zhou, R. J. Adrian, S. Balachandar, T. M. Kendall, Mechanism for generating coherent packets of hairpin vortices in channel flow, *J. Fluid Mechanics*, **387**, pp. 353-396, 1999.
[4] R. J. Adrian, Hairpin vortex organization wall turbulence, *Physics of Fluids*, **19**, 041301, pp. 1-16, 2007.
[5] S. Taneda, *Flow field visualization*, In F.I. Niordson and N. Olhoff (Eds.), Theoretical and applied mechanics (pp. 399-410), Amsterdam Elsevier Science, 1985.
[6] H. Dumitrescu, V. Cardos, I. Malael, Boundary vorticity dynamics at very large Reynols numbers, *INCAS BULLETIN*, vol. **7**, Issue 3, (online) ISSN 2247–4528, (print) ISSN 2066–8201, ISSN–L 2066–8201, DOI: 10.13111/2066-8201.2015.7.3.8, pp. 89-100, 2015.

[7] H. Dumitrescu, V. Cardos, A wave theory of incompressible fluid turbulence: wall elastic turbulence, *INCAS BULLETIN*, vol. **8**, Issue 2, (online) ISSN 2247–4528, (print) ISSN 2066–8201, ISSN–L 2066–8201, DOI: 10.13111/2066-8201.2015.8.2.4, pp. 41-51, 2016.
[8] M. J. Feigenbaum, Quantitative universality for a class of nonlinear transportations, *Journal of Stat. Phys*., **19**, pp. 25-52, 1978.
[9] M. O. Lorentz, Methods of measuring the concentration of wealth, *Publications of American Statistical Association*, **9**, pp. 209-218, 1905.
[10] W. I. King, *The elements of statistical method*, New York Macmillan, 1912.
[11] C. Gini, *Variability and mutability*, Ed. C. Cupini, Bologna, 1912.
[12] M. Gaster, A theoretical model of a wave packet in the boundary layer on a flat plate, *Proceedings of the Royal Society of London, Series A, Mathematical and Physical Science*, **347**, no. 1649, pp. 271-289, 1975.
[13] R. Jordinson, The flat plate boundary layer. Part 1 Numerical integration of the Orr-Sommerfeld equation, *J. Fluid Mech*, **43**, part 4, pp. 801-811, 1970.
[14] H. Dumitrescu, V. Cardos, Nearest Wall Flows – the Genuine Turbulence, *INCAS BULLETIN*, vol. **9**, issue 3, (online) ISSN 2247–4528, (print) ISSN 2066–8201, ISSN–L 2066–8201, DOI: 10.13111/2066-8201.2015.9.3.4, pp. 41-51, 2017.
[15] A. Tsinober, *The Essence of Turbulence as a Physical Phenomenon*, Springer Dordrecht Heidelberg, New York, London, 2014.